LABORATORY EXPERIMENTS AND MODAL MODEL OF IMPACT SOUND TRANSMISSION THROUGH A LIGHTWEIGHT WOODEN FLOOR

Yi Qin, Maarten Hornikx

Eindhoven University of Technology, Department of the Built Environment, Eindhoven, Netherlands. Email: y.qin@tue.nl

Susanne Bron, Arnold Koopman

Level Acoustics & Vibration BV, Eindhoven, Netherlands.

Lightweight floor systems are frequently used in many countries nowadays, but its poor acoustical performance is annoying for residents. This paper is concerned with low frequency impact sound transmission through a lightweight wooden floor. The floor system studied in this research consists of a ribbed wooden plate that is simply supported at its boundaries. A series of experiments on the lightweight wooden floor have been carried out in laboratory conditions. Besides, a modal analysis model is utilized to investigate the low frequency behaviour of this floor. This model is intended to be extended to evaluate improvements of the floor construction. The results of the measured floor vibrations and radiated sound field, for different excitation source types, are presented and compared with results from the prediction model. This paper gives insight in the behaviour of the floor excited by impact forces and the applicability of the model for predicting actual wooden floors.

Keywords: Lightweight floor, wooden floor, impact sound, modal analysis

1. Introduction

Although lightweight floors may offer convenience for construction and comfort for residents, the sound insulation is much lower than for heavyweight floors, especially at low frequencies. Due to the characteristics of the structure, these lightweight floors are apt to vibrate due to impact forces, like footsteps, dropped objects, and forces from household appliances such as washing machines. In addition, these vibrations can radiate noise to the room below the floor and reduce the sound quality of the indoor living environment.

The relationship between the impact sound transmission and characteristic lightweight floor structures has been investigated since these structures are increasingly used in both residential and non-residential buildings. Valuable efforts have been made in measuring vibrational features of lightweight floors [1] [2] and improving prediction methods of impact sound insulation [3].

This paper focusses on the investigation of a lightweight wooden floor system, and reports ongoing work in research towards an improvement of the impact sound insulation. As a starting point of this research, a laboratory measurement of this floor structure has been made and the measurement results are compared with an analytical solution, in order to understand the behaviour of the floor system and examine the agreement between measurement and prediction results. The analysis of the sound transmission, which is not much included in this paper, will be updated in a subsequent paper.

2. Measurement procedure

Measurements are conducted to investigate the vibration behaviour of a typical lightweight wooden floor, which is built in the acoustics laboratory at Eindhoven University of Technology. The measurement results will give validation for an analytical prediction method of lightweight structures and provide information of this basic structure for a future study towards improvement of its impact sound insulation. During the measurement, the floor was excited by using an impact hammer. The impulse response of the vibrational field of floor and acoustical field in the lower room are measured.

A 3.35 x 3.35 m simplified wooden floor was built in the acoustics test chamber, see Fig. 1. For the top plates, plywood with a thickness of 17 mm was used. Due to the limitation of the room entrance dimensions, it was impossible to carry in a single wooden plate that could cover the whole area of the floor. Therefore, 6 smaller pieces of plywood plate were used instead, joining together by flat-fell seams and screwed to the beams. The beams have a height of 190 mm and a width of 40 mm and are equally spaced at a distance around 412.5 mm from each other.

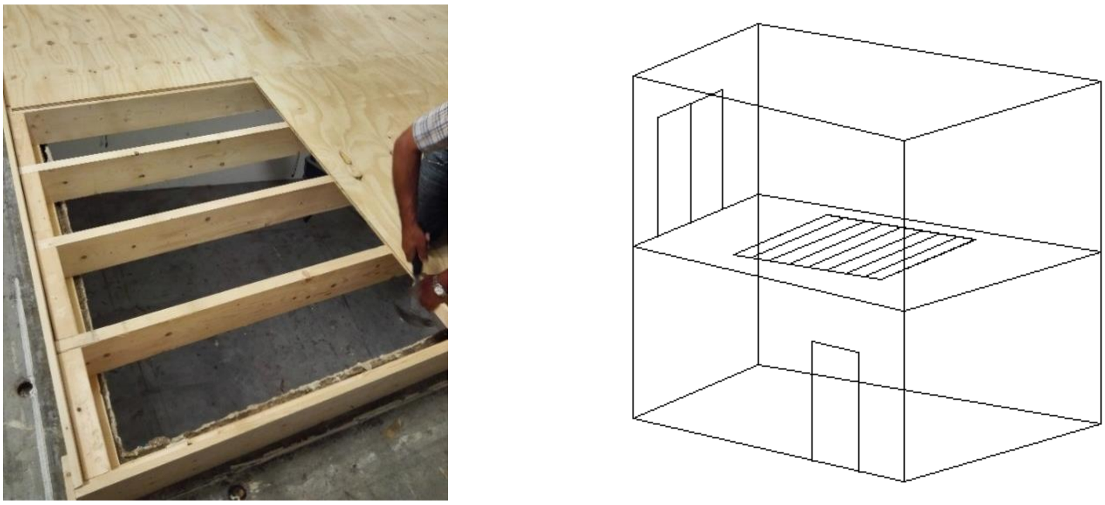

(a) (b)

Figure 1: Measured lightweight floor system.
(a) Picture of the floor during construction, (b) Schematic diagram of the floor in the laboratory.

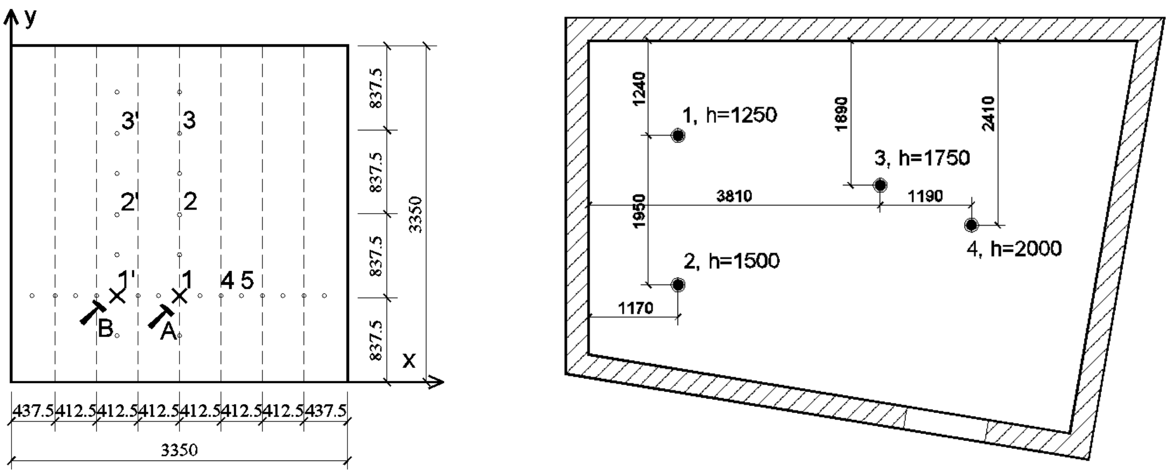

(a) (b)

Figure 2: The positions of the sensors for the impact sound measurement. Distance in (mm)
Positions of (a) accelerometers and sources on the floor, (b) Microphones in the receiving room.

Two force positions are used, see Fig. 2a. One is at (1.68m, 0.84m), around the ¼ beam length position in the middle of the floor, and the other is at (1.06m, 0.84m), between the 3rd and 4th beams. In order to excite the modes of the lightweight structure without making too much deformation at the driving point, which may induce non-linear effects in the system, only a small force is exerted on the floor by the hammer for each impact.

Accelerometers are distributed on the floor surface along the directions parallel to the beams and perpendicular to the beams. In the direction parallel to the beams, the accelerometers are distributed on the nodes every 1/8 beam length. In the other direction perpendicular to the beams, sensors are located in between and op top of the beams.

At the same time, 4 microphones are used to measure the sound radiated to the lower room, see Fig. 2b. The signals of the force, vibration and sound pressure are recorded simultaneously by a 24-channel NI data logger at a speed of 51.2 kHz for each channel, and the phase difference between the signals can be neglected.

3. Prediction method

Due to the capability of providing good insights into the low-frequency natural modal behaviour of a structure with a regular shape, Brunskog's Fourier series method [4] is selected to provide the analytical solution of the floor system. This method is developed to predict the velocity field of a floor structure supported by parallel beams, as our floor. The method is based on the thin plate theory and the Euler beam theory.

For a single plate excited by an external force, the bending wave equation for a monochromatic wave is

$$D_p\left(\frac{\partial^2}{\partial x^2}+\frac{\partial^2}{\partial y^2}\right)^2 w(x,y) - m_p\omega^2 w(x,y) = F(x,y), \qquad (1)$$

where D_p is the bending stiffness of the plate, w is the vertical displacement, ω is the angular frequency, m_p is the mass per unit area, and F is the external force. The bending wave displacements for a plate and for a beam are written as a summation of the contributions from the natural modes.

$$w_p(x,y) = \sum_{n=1}^{\infty}\sum_{m=1}^{\infty} c_{p,mn}\varphi_m(x)\psi_n(y), \qquad (2)$$

$$w_b(x_j,y) = \sum_{n=1}^{\infty} c_{b,jn}\psi_n(y), \qquad (3)$$

where c are the Fourier coefficients, w are the displacements, m are the mode numbers in x directions, which is from 1 to M, n are the mode numbers in y directions, which from 1 to N, and φ, ψ are the mode shapes along x and y directions, which are given by sine series respecting simply-supported boundary conditions.

$$\varphi_m(x) = \sqrt{\frac{2}{L_x}}sin(k_m x)\ , \quad \psi_n(y) = \sqrt{\frac{2}{L_y}}sin(k_n y). \qquad (4)$$

The movements of the plate and beam are equal at each beam position, $w_p(x,y) = w_b(x,j)$. In terms of Fourier coefficients, the plate and beams can be coupled as:

$$c_{b,jn} = \sum_m c_{mn}\varphi_m(x_j). \qquad (5)$$

In order to make use of matrix notations and algebra, the Fourier coefficients for the plate and beams are organized as vectors. By using a matrix $\boldsymbol{J}$, the coefficients can be coupled as $\boldsymbol{c_b} = \boldsymbol{J}\cdot\boldsymbol{c}$.

By considering the rotational kinetic energy from twisting beams, the torsion of the beams can also be incorporated into the model by:

$$c_{b,jn}^{r} = \frac{\partial}{\partial x} \sum_m c_{p,mn} \psi_n(y)\, \varphi_m(x_j). \tag{6}$$

Let a coupling matrix $\boldsymbol{L}$ be defined as $\boldsymbol{c_b^r} = \boldsymbol{L} \cdot \boldsymbol{c}$. The bending wave equation of the floor structure can now be solved as an eigenvalue problem of a forced vibration system:

$$(\boldsymbol{K} - \boldsymbol{M}\omega^2)\boldsymbol{c} = \boldsymbol{F}. \tag{7}$$

The diagonal matrixes of stiffness and mass for the coupled system are finally defined as [5]:

$$\begin{aligned} \boldsymbol{K} &= \boldsymbol{K_p} + \boldsymbol{J^T K_{b,F} J} + \boldsymbol{L^T K_{b,R} L}, \\ \boldsymbol{M} &= \boldsymbol{M_p} + \boldsymbol{J^T M_{b,F} J} + \boldsymbol{L^T M_{b,R} L}, \end{aligned} \tag{8}$$

where $\boldsymbol{K}$, $\boldsymbol{M}$, are MN ×MN matrixes. The unknown coefficient vector $\boldsymbol{c}$ and force vector $\boldsymbol{F}$ are both MN×1 dimensional. For a point force with amplitude Q, the force vector is denoted as:

$$\boldsymbol{F} = \boldsymbol{Q} \begin{bmatrix} \vdots \\ \boldsymbol{\varphi_m(x_0)\psi_n(y_0)} \\ \vdots \end{bmatrix}. \tag{9}$$

The velocity of the plate is now obtained by solving the coefficients $\boldsymbol{c}$ in Eq. 7 and then using Eq. 2. The method is implemented and solved in MATLAB.

4. Results

Figure 3 shows the shape of the measured signals in the time domain. The impact hammer firstly gives a transient impulse to the system. The vibrational response of the structure is detected by the accelerometer immediately. After a small delay of around 10ms the radiated sound reaches the microphone position. In frequency domain as shown in Fig. 3b, the force does show a rather flat distribution in low frequency range. In contrast, modal effects in the frequency response signals for the floor and room can be clearly observed.

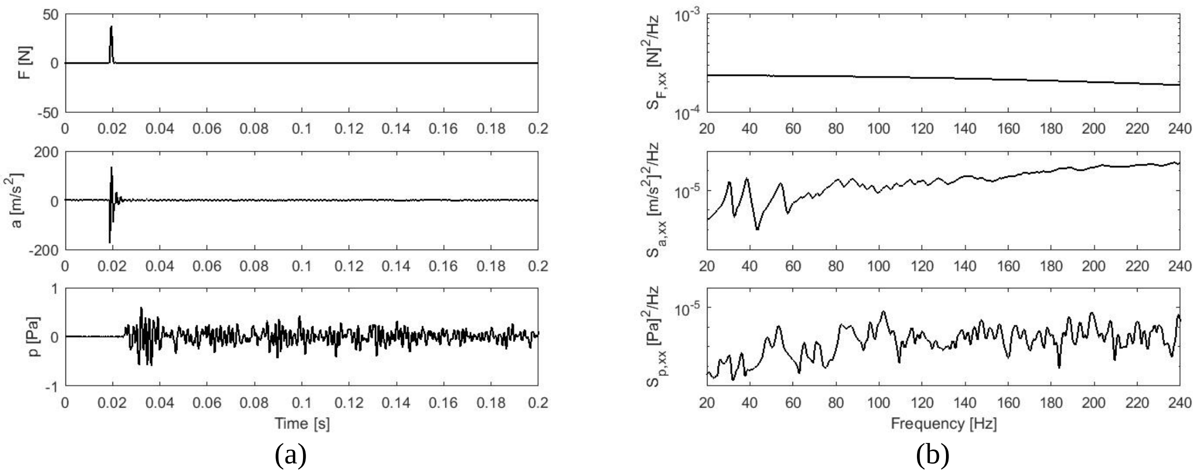

Figure 3: An example of measurement results for the force, acceleration and sound pressure.
Excitation point is at A; the accelerometer position is at 2; the microphone is at 3.
(a) Signals in Time domain, (b) Power spectrum density.

The transfer mobilities were measured and averaged between 6 hits for each accelerometer position. Figure 4 shows the measured point mobilities for the low frequency range from 20 to 240 Hz. The curves show larger fluctuations below 100 Hz, because the first modes are in this range. As the frequency increases, the modal density increases exponentially, the peaks for natural modes become closer. Also, damping at high frequencies to a larger extent influences the modal behaviour. Thus, in the frequency range above 140 Hz, the frequency for each individual mode is difficult to be detected directly from the figures.

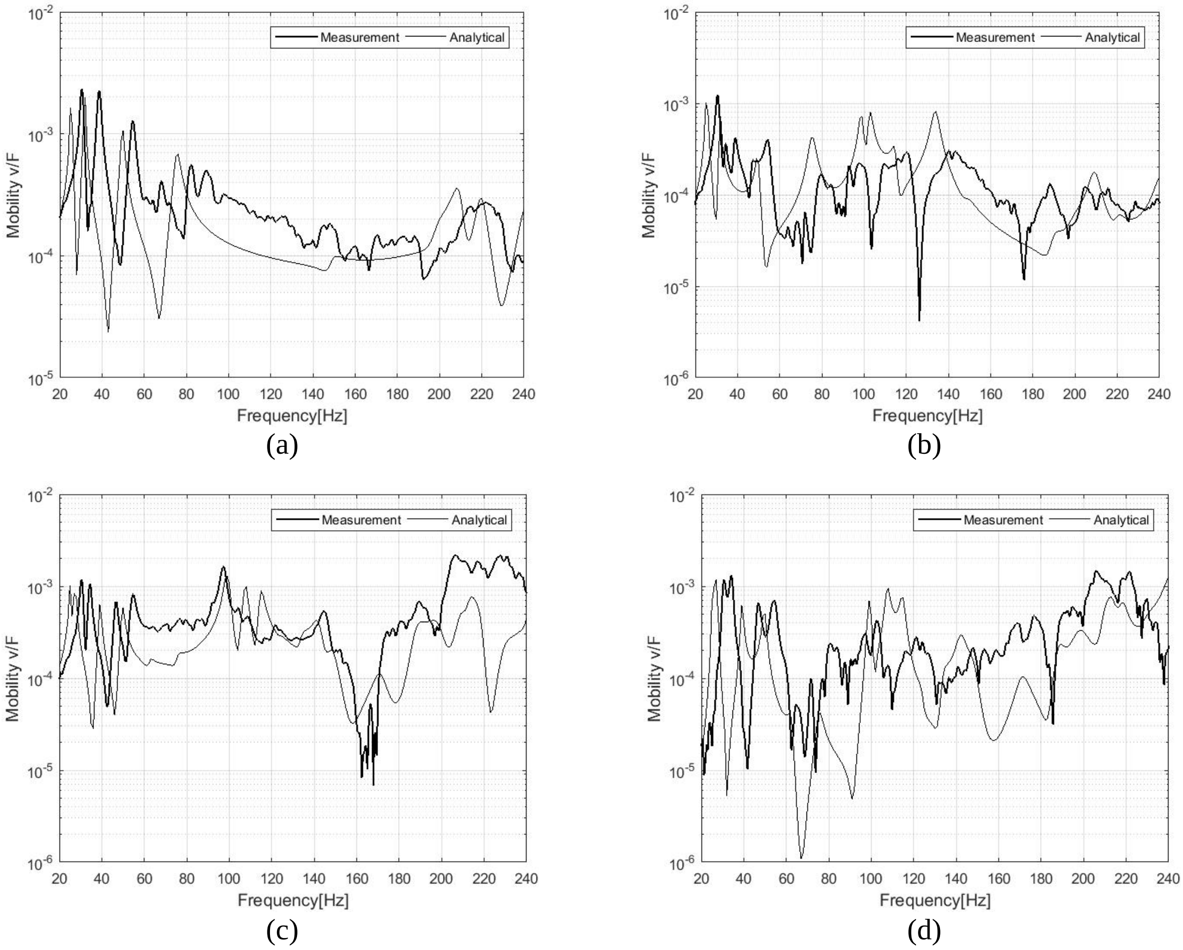

Figure 4: Transfer mobility obtained from measurements and the analytical method from section 3. (a) V(2)/F(A), (b) V(4)/F(A), (c) V(3')/F(B), (d) V(5)/F(B)

Also shown in Fig. 4 are the predicted values using the analytical method. In the predictions, the modulus of elasticity was assumed 5GPa for the plate, which is the averaged values of the measured two-directional Young's moduli of the same plate, and 13Gpa for the beams by taking the property of 'spruce' as a reference from [6]. The density was measured as 600 and 700 kg/m3 respectively. The Poisson's ratio was assumed as 0.4 for both the plate and the beams. A loss factor of 0.03 is introduced to consider structural damping of both materials.

In the analytical solutions, the plate is assumed as a simply-supported plate ribbed by 7 load-bearing beams; in contrast to the measured scenario no beams are considered on all edges. The mode number are set to be M = 30, N = 15. The bending wave velocities of the surface in z-direction are simulated and used to calculate the mobilities for each receiving point.

The measurement results show a similar shape as the predicted curves. The peaks have a better match with the predicted result at low frequencies, but the predicted natural frequencies are shifted to the lower frequencies.

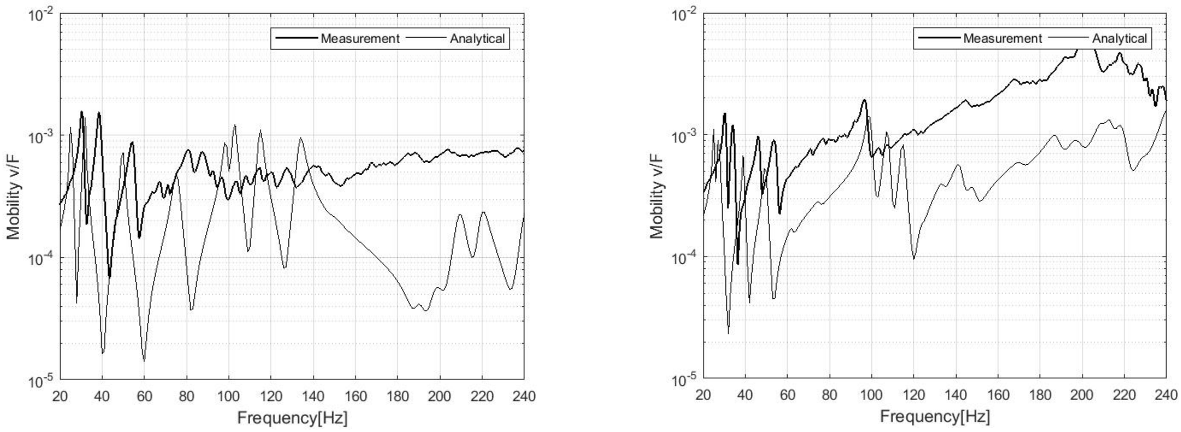

(a) (b)

Figure 5: Driving-point mobility obtained from measurements, analytical method from section 3 and FEM. (a) V(1)/F(A), (b) V(1')/F(B).

A high discrepancy is found between the amplitude of the measured and predicted driving-point mobilities, as shown in Fig. 5. The measured mobility is about 10 times larger than the predictions for the higher frequencies in Fig. 5b. For providing better prediction results at the driving point, a deeper understanding of the local effect caused by the hammer tips and floor material is needed.

Table 1: The eigen frequencies obtained from measurements and the analytical method.

Mode (m, n)	Measurement [Hz]	Analytical method [Hz]
1, 1	30.4	25.4
2, 1	34.8	27.4
3, 1	38.7	31.7
4, 1	54.7	39.1
5, 1	61.7	49.6
6, 1	71.1	62.4
7, 1	78.5	75.4
1, 2	97.7	98.7
2, 2	108.6	99.8
3, 2	114.6	102.6

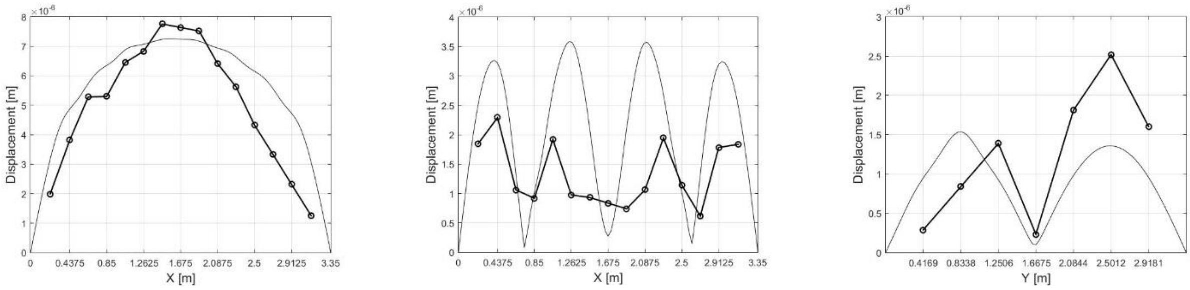

(a) (b) (c)

Figure 6: Mode shapes obtained by the measurement and the analytical method.
(Solid thick) measured, (Solied thin) analytical method.
(a) Mode 1, 1, (b) Mode 4, 1, (c) Mode 1, 2.

Table 1 shows the comparison between the measured natural frequencies and the predicted natural frequencies for the floor structure. The measured natural frequencies are higher than the values estimated with the analytical method. The measured mode number of the natural frequencies were determined by comparing the mode shapes with the predicted mode shape, see Fig. 6. The deflections of the plate at different natural frequencies show an agreement with the predicted mode shapes, which indicates they are caused by the same natural frequencies.

5. Discussion

Results of the measurement show differences from the predicted results. There are several possible reasons for these differences.

As the elastic modulus of the beam is larger than that of the plate, the natural modes along the beam direction such as (1,1), (1,2), significantly depends on the stiffness of the beams. In the prediction, the same material properties are used for all beams. Variations of the stiffness and mass for different beams may cause discrepancy between measured and predicted results.

On the other hand, the natural modes in direction perpendicular to the beam largely depend on the properties of the plates, for example the modes (2,1), (4,1). In the analytical method, the plate is assumed to be isotropic. A better result could be expected if an orthotropic plate is assumed and more accurate properties are determined.

In addition, the boundary condition in the measurement setup could be more complex than an exactly simply-supposed. The point connections of nails between the plates and beams could also have potential influence on the natural frequencies of the whole system.

6. Conclusions and future work

In this paper, the results of a laboratory measurement of a simplified lightweight floor system and predictions from an analytical method are presented as the initial work in research towards improvement of the impact sound transmission of this lightweight floor system.

The analytical prediction helps to get a better understanding of the vibration behaviour of the floor structure. In order to improve the accuracy of the prediction, the directionality of the wooden material will be taken into account and properties of materials should be examined more specifically such as the elasticity modulus. Further, a 3D numerical method solving the linear elasticity equations will be used to predict the mobilities of the floor system to verify the validity of the assumptions underlying the used analytical model [7]. Furthermore, it will be used to inspect the impact of different boundary conditions on the results. The results of this analytical model will be used for the sound radiation prediction and it will be extended to modifications of the floor system in order to investigate possible ways to lower the impact sound transmission through this lightweight floor system.

In further research, a different excitation force, a heel-drop of a human body, will be introduced. A heel-drop test device is designed for measuring forces and moments imposed on the floor system.

REFERENCES

1 Johansson, C. Low-frequency impact sound insulation of a lightweight wooden joist floor, *Applied Acoustics*, **44**(2), 133-147, (1995).

2 Emms, G. Low-frequency vibration measurements on LTF floors, *Proceedings of Inter-Noise 2006*, Honolulu, Hawaii, USA, 3-6 December, (2006).

3 Brunskog, J., and Hammer, P. Prediction Models of Impact Sound Insulation on Timber Floor Structures; A Literature Survey, *Building Acoustics*, **7**(2), 89-112, (2000).

4 Brunskog, J., and Chung, H. Non-diffuseness of vibration fields in ribbed plates, *the Journal of the Acoustical Society of America*, **129**(3), 1336-1343, (2011).

5 Dickow, K. A., Brunskog, J., and Ohlrich. M. Modal density and modal distribution of bending wave vibration fields in ribbed plates, *the Journal of the Acoustical Society of America*, **134**(4), 2719-2729, (2013).

6 Kollmann, F. P., and Cote, Jr, W. *Principles of Wood Science and Technology, I, Solid Wood*, Springer-Verlag New York Inc., (1968).

7 Sihar, I., Hornikx, M. and Pranowo. Time-domain structural vibration simulations by solving the linear elasticity equations with the discontinuous Galerkin method, Proceedings of the International Congress on Sound and Vibration, London, UK, 23-27 July, (2017).